17th Brazilian Congress of Thermal Sciences and Engineering
November 25th-28th, 2018, Águas de Lindóia, SP, Brazil

ENCIT-2018-0266
THERMAL ANALYSIS OF A VARIABLE CAPACITY COMPRESSOR FREQUENCY INVERTER

Maria Eduarda Chiamulera
Thyane Fuhrmann Gonçalves de Oliveira
César José Deschamps
POLO Research Laboratories for Emerging Technologies in Cooling and Thermophysics
Federal University of Santa Catarina, 88040-900 Florianópolis, Brazil
maria.chiamulera@polo.ufsc.br
thyane.oliveira@polo.ufsc.br
deschamps@polo.ufsc.br

Abstract. *Due to technology advancements, the power density of electronic components has considerably increased in recent years. However, high temperatures can affect the reliability of electronic components and, therefore, thermal analysis should be done as early as possible in the overall design process. The present paper reports a simulation model developed to predict the temperature distribution of the electronic components of a variable-frequency drive used in refrigeration compressors. A commercial computational software was adopted in the analysis and the results were validated through comparisons with experimental data of temperature in different components under three operating conditions.*

Keywords: *frequency inverter, thermal modeling, thermal management*

1. INTRODUCTION

Vapor compression refrigeration systems account for nearly a third of the total energy consumption in Brazilian residences (Eletrobras, 2016). In order to increase the compressor efficiency, variable speed technology has been applied to the electric motor. This allows the refrigeration system to operate with different cooling capacities according to the thermal load, resulting in lower energy consumption and better temperature control.

Variable-frequency drives (VFDs), also known as frequency inverters, control the motor speed by varying motor input frequency and voltage. VFDs have three main components: (i) rectifier, used to convert input alternating current (AC) into direct current (DC); (ii) DC bus, which stores and smoothens the incoming power; (iii) inverter, which uses pulse width modulation (pwm) to simulate a current sine wave at the desired frequency to the compressors motor. Due to safety requirements as well as to its exposure to hostile environments, the components of the VFD are usually placed inside a sealed plastic enclosure, resulting in limited or non-existing air circulation. Furthermore, in recent years, power electronics technology has shown a clear tendency of reducing the size of electronic devices. However, this has increased heat generation per unit area of the components, which increase considerably the temperature of the electronic equipment.

The operation of electronic components at high temperatures is a common cause of failure of electronic devices and a critical issue to improve the design of electronic packages. According to Wang *et al.* (2013), 55% of the failures in electronic devices occur due to temperature, 20% due to vibrations, 19% due to humidity and 6% due to the presence of dust. In fact, the reliability of electronic components is reduced exponentially as the operating temperature rises (Hu *et al*., 2005) and hence, it is very important to determine their operating temperatures.

Macarios and Barbosa (2014) measured the temperature of the components of a variable capacity compressor frequency inverter using infrared (IR) thermography. The images from the IR camera revealed a strong thermal interaction between components. Although this method requires the determination of surface emissivity of components, temperature results agreed within ±3 °C with measurements taken using type T thermocouples.

While measurements usually provide reliable data, CFD simulation has proven to be a very useful tool for thermal analysis of electronic equipment (Lee *et al*, 1995). The ANSYS Icepak is a commercial software developed for this purpose, solving the coupled fluid dynamics/heat transfer problem typical of electronic systems. For instance, Guofeng *et al.* (2013) developed a thermal simulation model of a sealed vehicle electronic controller using Icepak. The model was validated by comparing its predictions with experimental data, showing deviations smaller than 6 °C. After this validation, the authors studied the impact of factors that influence the maximum temperature of the printed circuit board (PCB), such as the case height, board construction and component positioning. Simulation results showed that doubling the copper coverage area (due to the circuit traces) on the PCB layers can reduce the board temperature by 15 ºC.

Harvest *et al.* (2007) investigated the thermal effect associated with the spacing between the components of a PCB. Using a numerical model validated via comparisons with experimental data, the impact of several parameters on the

operating temperature of the devices was studied including the board thermal conductivity. The authors concluded that there is a spacing from which each component reaches a temperature that is independent of distance. The results found in the parametric analysis showed that the conductivity of the PCB is one of the factors with the strongest effect on the device operating temperature. Moreover, the board with the highest thermal conductivity also resulted in the largest distance from which the components no longer interact thermally.

Similarly, Sawai *et al.* (2012) developed a simulation model to predict heat transfer in sealed airborne electronic equipment. The study was focused on the comparison of four different types of PCB according to its thermal conductivity due to copper content, varying from a simplified uniform material to a detailed copper trace pattern of each layer. As expected, the improvement of design precision increased the accuracy of the calculation result for the temperatures, yielding a maximum error of 5%. However, the detailed model requires longer simulation time compared to the first representation. They also compared the design costs with and without thermal simulation, proving the effectiveness and the importance of thermal simulation methods in the development process.

Gao *et al.* (2013) conducted a numerical study to predict the temperature and airflow distribution within an avionics equipment. An analysis was performed to determine the importance of the different heat transfer mechanisms that takes place in the PCB: conduction, natural convection and radiation. The authors concluded that conduction was the most important heat transfer mechanism, representing more than 50% of the total heat flux of the circuit board.

Sardana *et al.* (2016) simulated an electronic control unit exposed to climatic conditions such as solar radiation in order to predict the temperature of its components. The equipment under analysis was sealed and comprised a battery and a PCB with components. Predictions of temperatures were compared to measurements and agreement was found to be in the range of ±5%. Modifications were proposed in the product orientation and battery positioning, without affecting its cost, resulting in a reduction of about 3 °C in the battery temperature.

This paper presents a simulation model developed to calculate the temperature distribution of electronic components on the PCB of a frequency inverter used in refrigeration compressors. First, the assumptions and boundary conditions of the simulation model are detailed. The results are then compared with experimental data for temperature. Finally, modifications are proposed and discussed for the model.

2. METHODOLOGY

The Variable-frequency drive (VFD) analyzed in this study is attached to the external surface of the compressor shell. It is a vertically oriented PCB with the electronic components inside a nearly sealed enclosure. An aluminum heat spreader is positioned on one side of the board and a thermal adhesive is used to integrate components and the heatsink. In this analysis, only the most dissipative components and those that can affect the airflow inside the enclosure were considered. Figure 1 shows a schematic representation of the board and Tab. 1 indicates the highest power dissipated per unit surface area of the components. ICs correspond to integrated circuits.

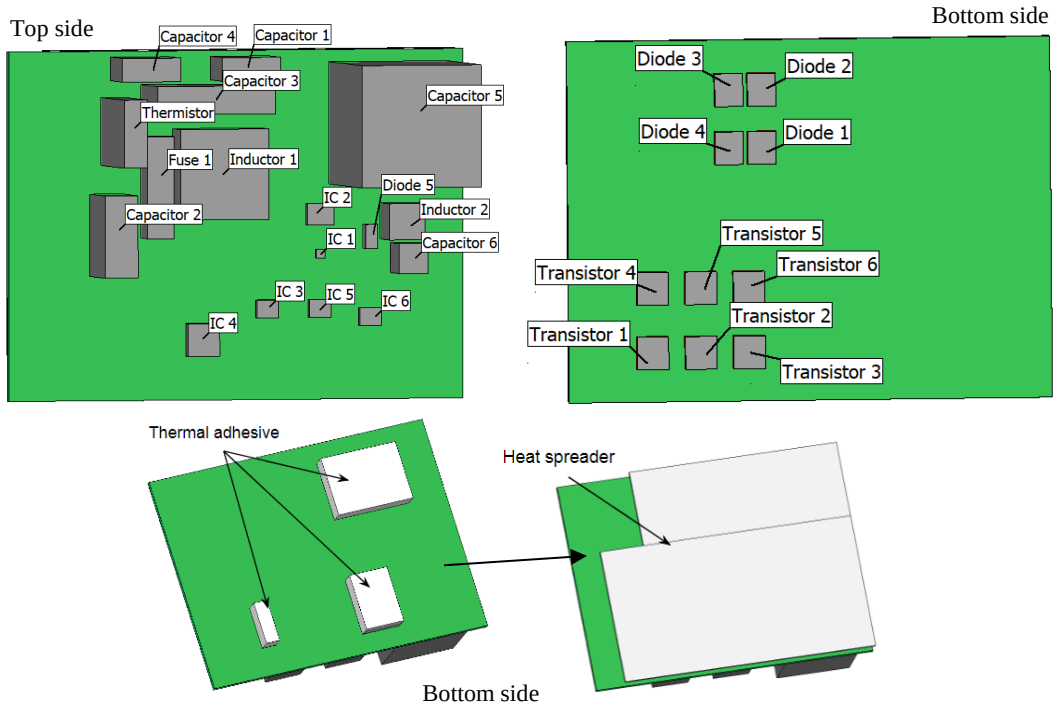

Figure 1. Circuit board layout and thermal adhesive and heat spreader positioning.

The electronic components were modeled as solid blocks with isotropic thermal conductivity and the PCB was modeled as a homogeneous solid material with bi-directional thermal conductivities (planar and normal).

Table 1. Highest heat dissipation per unit area of the frequency inverter components.

Component description	Heat flux (W/cm^2)
Integrated Circuit (IC1)	1.900
Transistor 4 (T4)	0.978
Transistor 1 (T1)	0.677
Diode 1 (D1)	0.236
Thermistor (Th)	0.182

The orthotropic thermal conductivity of the board material was calculated based on the conductor volume fraction in the PCB as follows, according to Ellison (2011):

$$k_{in-plane} = \left(\frac{A}{100} \cdot k_c\right) + \left(1 - \frac{A}{100}\right) \cdot k_d \quad \text{and} \quad k_{through-plane} = \left(\frac{\frac{A}{100}}{k_c} + \frac{1-\frac{A}{100}}{k_d}\right)^{-1}, \tag{1}$$

where A is the percentage of conductor material in the PCB, k_c is the thermal conductivity of copper and k_d is the thermal conductivity of the dielectric material, FR4. Table 2 shows the resulting thermal conductivity calculated for the board.

Table 2. Thermal conductivity for the inverter PCB.

% conductor by volume: 11.6%	Orthotropic thermal conductivity
$k_{copper} = 385\ \mathrm{W/m \cdot K}$	$k_{in-plane} = 44.9\ \mathrm{W/m \cdot K}$
$k_{FR4} = 0.3\ \mathrm{W/m \cdot K}$	$k_{through-plane} = 0.34\ \mathrm{W/m \cdot K}$

In order to reduce computational processing cost, the complex geometry of the VFD plastic enclosure was simplified as a rectangular box with the same overall dimensions and separated by a distance of 10 mm from the compressor wall. The compressor wall was set with a fixed temperature boundary condition of 85 °C and the temperature of the ambient air surrounding the VFD was set to 55 °C. These values represent the worst-case operating scenario for the VFD. Figure 2 shows the whole solution domain as well as the inverter orientation and geometry. According to Fig. 2, the boundaries of the domain are: ±z, -x and -y set as openings and +x and +y set to walls. Gravity vector is aligned with the x+ axis.

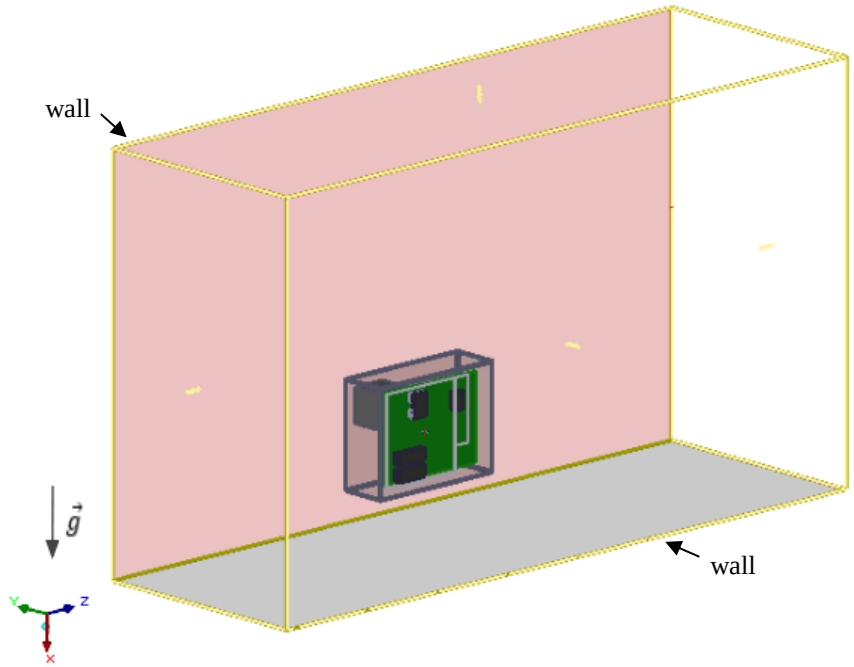

Figure 2. VFD thermal simulation model.

Initially, the numerical results were verified concerning truncation error via mesh refinement. Hence, the mesh was refined up to the level from which the temperatures of the components varied less than 1%. Figure 3 illustrates the influence of mesh refinement on the temperatures of some components (Diode D1, Capacitor C1, Capacitor C6, Transistor T1, Thermistor Th, Integrated circuit IC1) of the PCB. It is observed that meshes with more than 1.5E+6 elements predict virtually the same temperatures. In conclusion to the study, a hex-dominant unstructured mesh with 1,786,956 elements was chosen to discretize the computational domain.

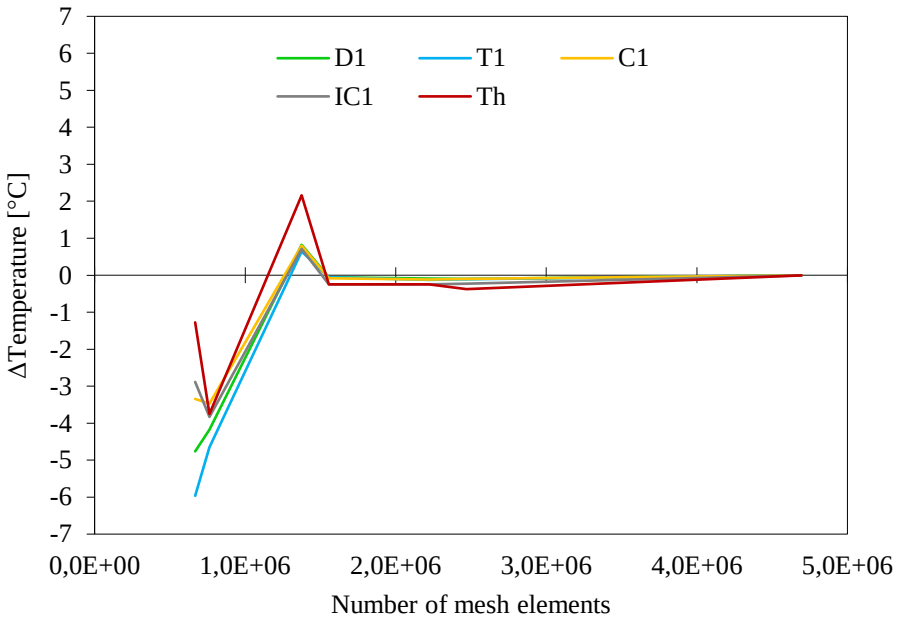

Figure 3. Mesh independence study.

The simulation model adopted a three-dimensional steady-state heat and fluid flow formulation. Icepak estimated the Rayleigh number and Prandtl number as 3.59E+7 and 0.708, respectively, representing laminar natural convection. Thermal radiation on all exposed surfaces of each component was considered via the surface-to-surface model, which calculates the form factor of the surfaces.

3. RESULTS AND DISCUSSION

Experimental data for the temperature of the components were measured using thermocouples with an uncertainty of ±2 °C. The temperature of the plastic enclosure was measured at the middle point of the surface facing the environment (-y). A thermocouple was also placed inside the inverter box to measure the internal air temperature. The temperatures were predicted at the same positions in which the thermocouples were placed.

The differences between the measured, T_M, and predicted, T_P, temperatures for the frequency inverter in a given operating condition (motor @1300 rpm) are shown in Fig. 5 (referred as simplified). As can be observed, the results are similar to the measurements, with differences smaller than 15 °C. However, in general the simulation model underestimated the temperatures of the frequency inverter. This may be due to the fact that the enclosure surface geometry next to the compressor has some protrusions not considered in the previous analysis. These protrusions include an "opening" to the compressor where the wires from the inverter are connected. Therefore, the enclosure geometry adopted in the model was modified to include these features so as to investigate their impact on the heat transfer.

3.1 Influence of enclosure geometry

As mentioned, the first analysis was carried out with a simplified enclosure representation. Figure 4 shows the geometric changes for the enclosure in order to represent the protrusions for the wiring connection with the compressor fence and an extended surface for the capacitor housing. The results are shown in Fig. 5 and the differences between measured, T_M, and predicted, T_P, temperatures are compared for the simplified and the modified enclosure geometry. It can be observed that, in general, the geometric improvements in the enclosure decreased the temperature difference between measured and predicted. As expected, an increase in the temperature of the components occurred by the direct contact between the internal air and the hot compressor wall, altering the heat transfer inside the enclosure.

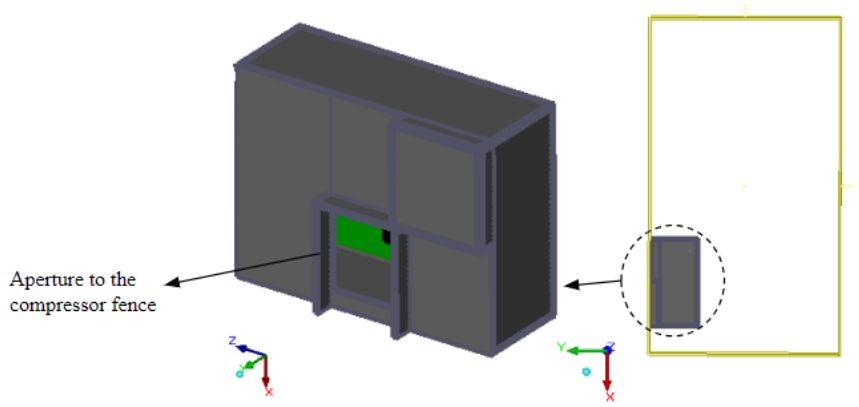

Figure 4. Modified geometry of the enclosure and positioning on domain.

As shown, the correct representation of the contact between the enclosure and the compressor wall is essential for predictions in close agreement with measurements. However, even though the predictions of temperature for most of the components was in better agreement with the experimental data, the predictions of some components were still not good enough, with the maximum difference reaching approximately 12 °C. Components such as IC3 and Transistor T6 have their location nearly mirrored relative to the board, and a possible reason for their temperature differences is due to the current PCB model that does not accurately represent heat transfer in the inverter.

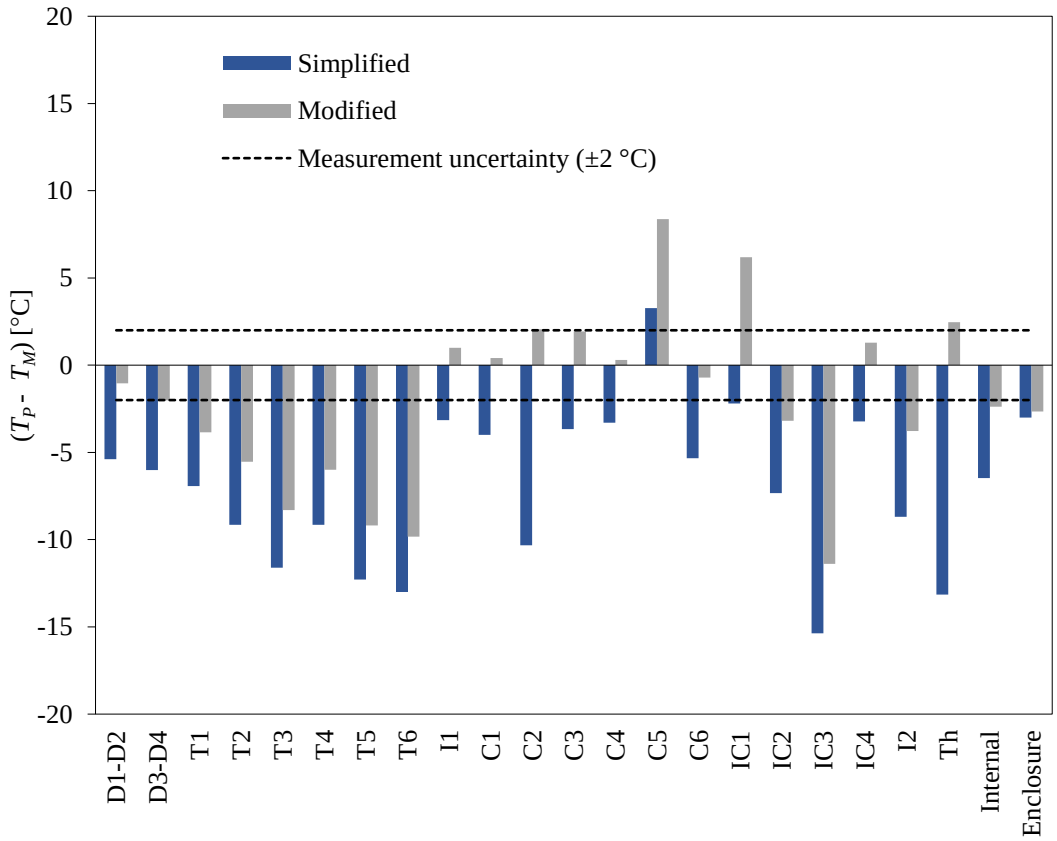

Figure 5. Deviations between predicted and measured temperature for the simplified and modified model.

3.2 Influence of the PCB representation

A further improvement in the simulation model was related to the board thermal modeling. Considering natural convection in a system of small size, the heat dissipated from the components is mainly transferred to the PCB via conduction, hence requiring a suitable modeling of the board. As previously mentioned, the VFD PCB is made of copper and FR4 material. While its representation as an orthotropic material takes into account the percentage of copper in the board, a locally varying thermal conductivity information on the board should be more representative. That can be done

by importing the traces locations on the PCB. The program then discretizes the board and calculates the thermal conductivity of each cell based on the presence of conductor or dielectric material. Figure 6 compares the differences between the measured, T_M, and predicted, T_P, temperatures for the PCB modeled as an orthotropic thermal conductivity and considering the circuitry information on the board layers. As can be seen, the incorporation of detailed information about the board construction allows closer agreement between predictions and measurements. Nevertheless, the temperature deviation of the integrated circuit IC1 increased approximately by 9 °C, reaching a deviation of almost 15 °C. This can be explained by inaccuracies in the positioning of this small size component concerning the traces on the board. Despite of that, the model resulted in temperatures within the measurement uncertainty in fourteen of the twenty-three points. Figure 7 shows the predicted temperature distribution of the components and PCB for this operating condition. As expected, the maximum temperature occurs in the integrated circuit IC 1 with a value of about 129 °C. High temperatures are also observed in the transistors and the thermistor, which are the components with the highest heat fluxes on the board.

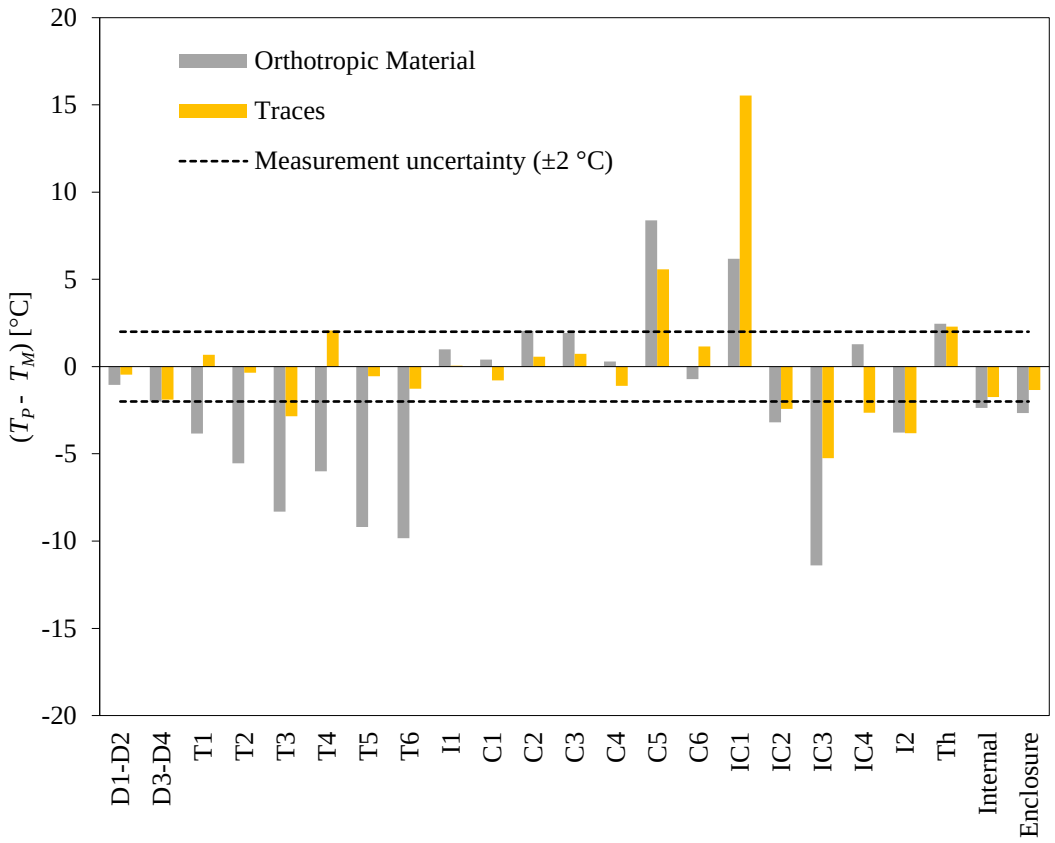

Figure 6. Deviations between predicted and measured temperature for different PCB models.

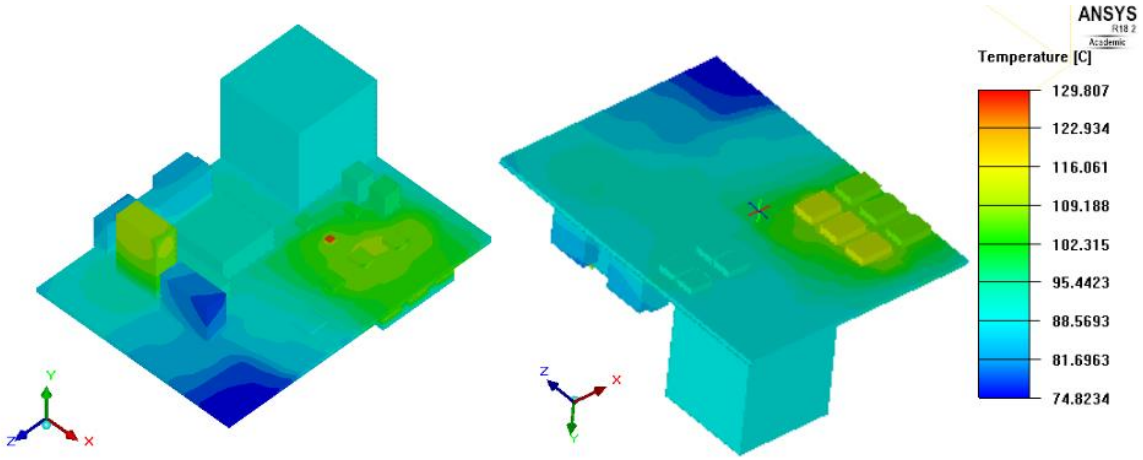

Figure 7. Predicted temperature distribution of the board and components surface.

Figure 8 compares the results of the simplified model (referred as baseline) and improved model for the temperatures of the components. The improved model predicts results in better agreement with the measurements and most of its predictions are within ±5% of difference. The remaining considerable differences between predictions and measurements are probably caused by incorrect input power consumption values or different monitor point location for the simulation temperature than the thermocouple position. In fact, the predictions show temperature gradients on the component surfaces. Overall, the model is able to predict reasonably the temperatures of the components.

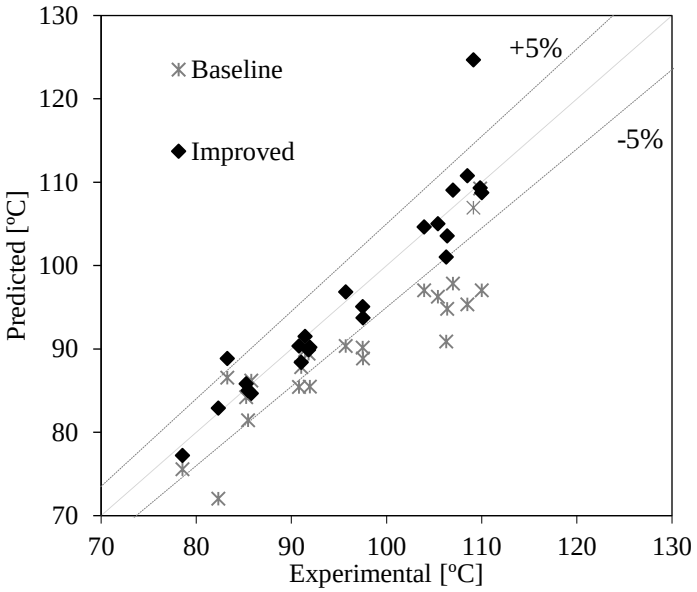

Figure 8. Comparison of predicted and measured temperatures for baseline and improved models.

3.3 Operating condition

The improved model was adopted to analyze the frequency inverter in three different operating conditions represented by the speed of the electric motor, which affects the power loss in some of the components. Figure 9 shows the deviations between predicted and measured temperature for the motor operating at 1300 rpm, 3300 rpm and 4500 rpm.

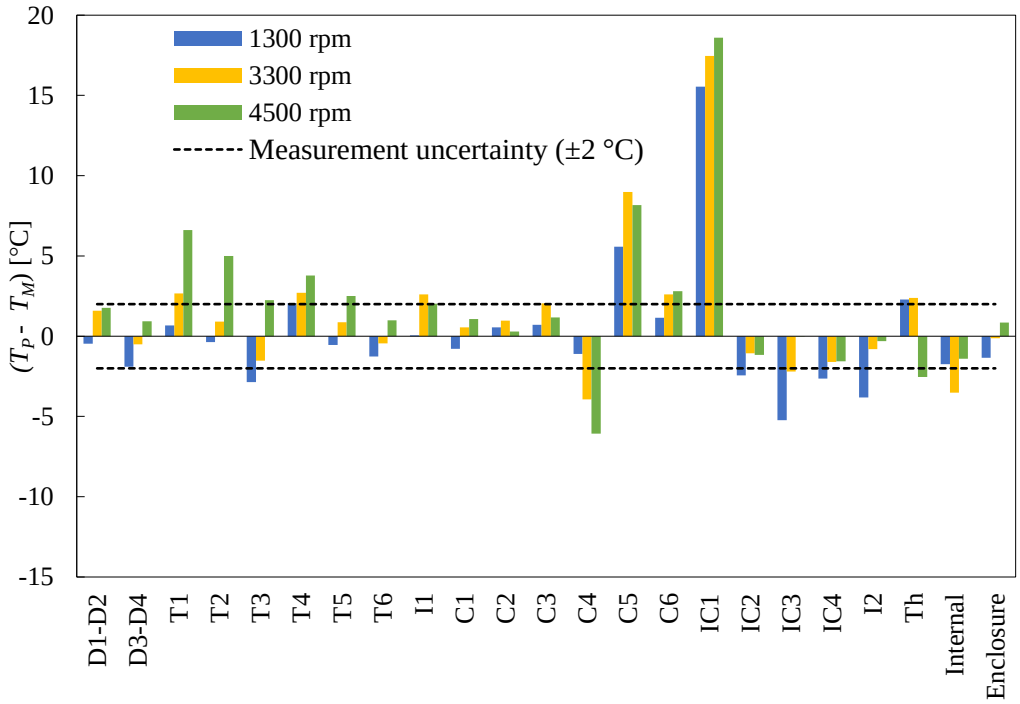

Figure 9. Deviations between predicted and measured temperature for different inverter operations.

As can be observed, the predictions for most of the components are within the uncertainty range of the measurements. The model tend to overestimate the temperature for the Capacitor C5 and the integrated circuit IC1 in all operating conditions. However, the model captures correctly the temperature trend for most of the components resulting from the different input power losses.

3.4 Heat transfer modes analysis

The electronic components of the inverter exchange heat through three modes: conduction, natural convection and radiation. In dissipative components, conduction is the main form of heat transfer. Devices such as transistors and diodes are bonded to the thermal adhesive, thus conducting nearly all power lost due to their inefficiencies to the board or the adhesive. In other high heat flux components, conduction to the board also accounts for large portion of the total heat dissipation. Figure 10 illustrates the heat dissipation by the three heat transfer modes for some of these components. Low-speed air flow takes place inside the enclosure, thereby the proportion of heat removal through convection is small. The surface areas of the integrated circuits IC3 and IC2 are approximately ten and five times greater, respectively, than that of IC1 and, therefore, heat transfer due to convection and radiation are more representative for these components.

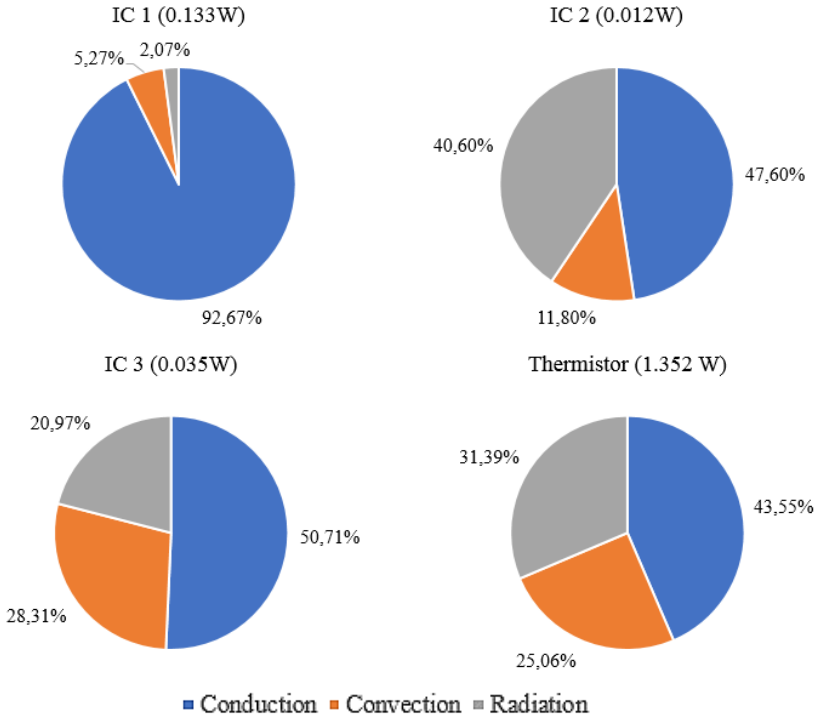

Figure 10. Heat dissipation by different heat transfer modes.

4. CONCLUSIONS

This paper presented a simulation model developed to predict the temperatures of the main components of a variable frequency-drive used in refrigeration compressors. Despite the simplifications adopted in the baseline model, the results were in reasonable agreement with experimental data. In order to reduce the differences between predictions and measurements, modifications were proposed with respect to the enclosure geometry and the board thermal model. A better modeling of the enclosure surface facing the compressor wall improved the predictions, indicating the importance of the thermal interaction between the air inside the inverter and the compressor wall. Two different representation of the PCB thermal conductivity were also studied. The model was successfully validated in different operating conditions and the heat transfer modes in different components were analyzed.

5. REFERENCES

ANSYS, Ins., ANSYS Icepak 2017. User's Guide. Release 18.2.

Eletrobras, 2016. "Dicas de Economia de Energia por Setor de Consumo". 28 Mar. 2018 <https://www.eletrobras.com/pci/main.asp>.

Ellison, G. N., 2011, "Thermal computations for electronics: conductive, radiative, and convective air cooling", 1 ed., CRC Press, Boca Raton, EUA.

Gao, H., Xiao, Z. and Xie, Y., 2013. “Numerical simulation of coupling heat transfer n sealed airbone electronic equipments”. *Applied Mechanics and Materials,* Vols. 275-277, p. 642-648.

Guofeng, R., Feng, T. and Lin, Y., 2013. “The research of thermal design for vehicle controller based on simulation”. *Applied Thermal Engeneering,* Vol 58, p. 420.

Harvest, J., Fleischer, A. S. and Weinstein, R. D., 2007, “Modeling of the thermal effects of heat generating devices in close proximity on vertically oriented printed circuits boards for thermal management applications”. *International Journal of Thermal Sciences,* Vol. 46, p. 253-261.

Hu, X. J., Padilla, A. A., Xu, J., Fisher, T. S. and Goodson, K. E., 2006. “3-Omega measurements of vertically oriented carbon nanotubes on silicon”. *Journal of Heat Transfer,* Vol. 128, p. 1109.

Lee, T.-Y.T.L., Chambers, B., Mahalingam, M., 1995. "Application of CFD technology to electronic thermal management". *IEEE Transactions on Components, Packaging, and Manufacturing Technology: Part B,* Vol. 18, p. 511.

Macarios, T. C. and Barbosa, J. R., 2015. “Infrared thermal imaging analysis of a 1-kW variable capacity compressor frequency inverter”. *Journal of the Brazilian Society of Mechanical Sciences and Engeneering,* Vol. 37, p. 275.

Sawai, Y., Hirahata, K., Yokota, M., Okayama, A., Sawada, M. and Hagihara, S., 2012. “Applications of simulation technology of thermal issues”. *Application of Simulation Technology to Thermal Issues,* Vol. 74, p. 78.

Sardana, N. K., Pattnayak, R. A., Busam, S. P. K., Ghosh, C. K. and Biswal, L., 2016, “Thermal analysis of a battery in an electronic device for an outdoor application”. ICEP 2016 Proceeding.

Wang H., Liserre, M. and Blaabjerg, F., 2013, “Toward Reliablle Power Electronics”., *IEEE Industrial Electronics Magazine,* Vol. 13, p. 17-26.

6. RESPONSIBILITY NOTICE

The authors are the only responsible for the printed material included in this paper.